ISPRS Journal of Photogrammetry and Remote Sensing 83 (2013) 94–103

Contents lists available at SciVerse ScienceDirect

ISPRS Journal of Photogrammetry and Remote Sensing

journal homepage: www.elsevier.com/locate/isprsjprs

Estimation of soil moisture using optical/thermal infrared remote sensing in the Canadian Prairies

Parinaz Rahimzadeh-Bajgiran [a,*], Aaron A. Berg [a], Catherine Champagne [b], Kenji Omasa [c]

[a] Department of Geography, University of Guelph, 50 Stone Road East, Guelph, ON N1G 2W1, Canada
[b] Agriculture and Agri-Food Canada, Ottawa, ON, Canada
[c] Department of Biological and Environmental Engineering, Graduate School of Agricultural and Life Sciences, The University of Tokyo, 1-1-1Yayoi, Bunkyo-ku, Tokyo 113-8657, Japan

ARTICLE INFO

Article history:
Received 5 November 2012
Received in revised form 19 June 2013
Accepted 19 June 2013
Available online 15 July 2013

Keywords:
Soil moisture
Evaporative fraction
Land surface temperature
Air temperature
MODIS

ABSTRACT

A new approach to estimate soil moisture (SM) based on evaporative fraction (EF) retrieved from optical/thermal infrared MODIS data is presented for Canadian Prairies in parts of Saskatchewan and Alberta. An EF model using the remotely sensed land surface temperature (Ts)/vegetation index concept was modified by incorporating North American Regional Reanalysis (NAAR) Ta data and used for SM estimation. Two different combinations of temperature and vegetation fraction using the difference between Ts from MODIS Aqua and Terra images and Ta from NARR data (Ts−Ta Aqua-day and Ts−Ta Terra-day, respectively) were proposed and the results were compared with those obtained from a previously improved model (ΔTs Aqua-DayNight) as a reference. For the estimation of SM from EF, two empirical models were tested and discussed to find the most appropriate model for converting MODIS-derived EF data to SM values. Estimated SM values were then correlated with in situ SM measurements and their relationships were statistically analyzed. Results indicated statistically significant correlations between SM estimated from all three EF estimation approaches and field measured SM values ($R^2 = 0.42$–0.77, p values < 0.04) exhibiting the possibility to estimate SM from remotely sensed EF models. The proposed Ts−Ta MODIS Aqua-day and Terra-day approaches resulted in better estimations of SM (on average higher R^2 values and similar RMSEs) as compared with the ΔTs reference approach indicating that the concept of incorporating NARR Ta data into Ts/Vegetation index model improved soil moisture estimation accuracy based on evaporative fraction. The accuracies of the predictions were found to be considerably better for intermediate SM values (from 12 to 22 vol/vol%) with square errors averaging below 11 $(\text{vol/vol\%})^2$. This indicates that the model needs further improvements to account for extreme soil moisture conditions. The findings of this research can be potentially used to downscale SM estimations obtained from passive microwave remote sensing techniques.

1. Introduction

Soil moisture (SM) is a critical factor in various environmental studies and is used as a key variable in several applications such as drought severity and duration, irrigation scheduling, soil erosion, evapotranspiration, forest fire hazard and forest management. Although direct measurement is the most accurate method for estimating soil moisture, this technique is expensive, time consuming and only provides point measurements. Therefore, in situ measurements may not represent the spatial distribution of SM and are not available for continuous spatial and temporal coverage at regional and global scales.

Technological advances in satellite remote sensing have offered an alternative to field measurements of SM and enabled us to monitor it at higher temporal and spatial resolutions at lower cost and time. Since the 1970s a number of remote sensing methods have been developed to investigate soil moisture using different regions of electromagnetic spectrum from the optical to microwave regions (Carlson et al., 1995a; Gillies and Carlson, 1995; Jackson et al., 1976; Njoku, 1977; Sandholt et al., 2002; Schmugge, 1978; Schmugge and Jackson, 1994). Comprehensive reviews on the application of remotely sensed methodologies for the estimation of surface SM including the principles, advantages and constraints can be found in Carlson (2007), Moran et al. (2004), Owe et al. (2008), Verstraeten et al. (2008), Wang and Qu (2009).

The main disadvantage of current methods to estimate SM from passive microwave techniques is the low spatial resolution (∼40 km) making it difficult to study sub-pixel variations in an

* Corresponding author. Tel.: +1 519 824 4120.
E-mail addresses: prahimzadeh@gmail.com (P. Rahimzadeh-Bajgiran), aberg@uoguelph.ca (A.A. Berg), Catherine.Champagne@AGR.GC.CA (C. Champagne), aomasa@mail.ecc.u-tokyo.ac.jp (K. Omasa).

0924-2716/$ - see front matter © 2013 International Society for Photogrammetry and Remote Sensing, Inc. (ISPRS) Published by Elsevier B.V. All rights reserved.
http://dx.doi.org/10.1016/j.isprsjprs.2013.06.004

appropriate manner (Merlin et al., 2010). Therefore, there is need for the development of approaches for downscaling SM data from low resolution microwave sensors. Optical/thermal remote sensing data provide finer resolution information that can be used to improve passive microwave estimations. Efforts are being made to downscale passive microwave SM estimations using optical/thermal infrared data (Chauhan et al., 2003; Merlin et al., 2010; Merlin et al., 2008; Piles et al., 2011) but downscaling methodologies still need to be improved.

Optical/thermal infrared sensing method known as Surface Temperature/Vegetation Index Method is a promising approach to estimate SM as surface temperature (Ts) and vegetation have been found to have a complicated dependence on SM. The application of approaches combining vegetation indices and the Ts dates back to the 70 s using the concept for detecting canopy water stress and crop evapotranspiration using aerial thermal scanners (Bartholic et al., 1972; Heilman et al., 1976). Later, using remote thermal sensing instruments, indices such as the Crop Water Stress Index (CWSI) were developed to be used for irrigation scheduling (Idso et al., 1981; Jackson et al., 1981). Over the past 40 years, the Ts/vegetation concept has been applied for various applications such as the estimation of evapotranspiration (ET), evaporative fraction (EF) and SM using Advanced Very High Resolution Radiometer (AVHRR), Landsat, MODerate resolution Imaging Spectroradiometer (MODIS) sensors, etc. A number of studies have documented the Ts/vegetation index (mainly NDVI) relationship and described the triangular shape of the data falling between the Ts and the NDVI axes (Carlson et al., 1995b; Gillies et al., 1997; Jiang and Islam, 2001; Nishida et al., 2003; Price, 1990; Venturini et al., 2004). Comprehensive reviews on the application of remotely sensed Ts/vegetation indices for the estimation of soil surface moisture and evapotranspiration can also be found in Petropoulos et al. (2009) and Li et al. (2009).

The application of the Ts/vegetation concept for SM estimation began with the work of Nemani et al. (1993) who found a strong negative relationship between Ts and Normalized Difference Vegetation Index (NDVI) for all biome types studied with a distinct change in the slope between dry and wet days. The idea was further developed by Carlson et al. (1995a), Carlson et al. (1995b) presenting the universal triangular method to explore relationships between SM, Ts and NDVI. Since then, a number of studies have suggested the application of Ts/vegetation concept for SM estimation (Gillies and Carlson, 1995; Mallick et al., 2009; Sandholt et al., 2002; Wang et al., 2011). The above mentioned studies mainly focused on direct estimation of SM from the Ts/vegetation index space.

Another potential, although not as well documented in the remote sensing literature, method to estimate SM is through the relationship between SM and evaporative fraction (EF). To do this, EF needs to be estimated and then transformed into SM values using empirical equations. Many water and energy balance models such as the bulk transfer (Deardorff, 1978) and Priestley–Taylor (Priestley and Taylor, 1972) models parameterized evaporation rate by the so-called surface moisture availability factors. As described by Lee and Pielke (1992), surface moisture availability factors are either α-type or β-type. While α-type models express the land surface moisture as the air relative humidity, β-type models also take onto account water transport from inner soil pores to soil surface. β-type models are easier to use than α-type ones as they are only a function of SM and wind speed (Kondo et al., 1990; Lee and Pielke, 1992). A number of empirical models ranging from simple linear to more sophisticated exponential and cosine models (Crago, 1996; Deardorff, 1978; Jacquemin and Noilhan, 1990; Komatsu, 2003; Kondo et al., 1990; Lee and Pielke, 1992; Noilhan and Planton, 1989) have been suggested to correlate surface moisture availability factors to SM at different soil depths. In the Priestley–Taylor model, α is equivalent to Priestley–Taylor coefficient and β is equivalent to EF (Davies and Allen, 1973; Crago, 1996).

As described above, because there is a relationship between EF and SM, it will be then possible to estimate SM from EF retrieved from remotely sensed data as well. A number of models have been developed to estimate EF using the Ts/vegetation index concept but they have been used for ET estimation (Jiang and Islam, 2001; Nishida et al., 2003). It has been found that EF is generally more stable during the day than evapotranspiration and therefore can be regarded to be a more suitable indicator of SM than ET (Yao et al., 2011). Remotely sensed EF data have already been shown to have strong correlations with field measured SM suggesting the possibility of SM estimation at a larger scale than laboratory experiments (Anderson et al., 2007; Wang et al., 2006). Recently, a similar concept was used to downscale passive microwave soil moisture data using the SM/EF relationship (Merlin et al., 2010; Merlin et al., 2008). However, not many studies on the development of sound models for the estimation of SM from remotely sensed EF are available.

Jiang and Islam (2001) estimated EF by using the Ts/vegetation index concept to calculate the Priestley–Taylor parameter and eventually ET using AVHRR data. The authors obtained satisfactory estimation accuracies with fewer number of input variables than the original Priestley–Taylor model. Further research (e.g. (Stisen et al., 2008; Wang et al., 2006)) evaluated improvements to the Jiang and Islam (2001) methodology. A different approach was taken by Nishida et al. (2003); their method used a two-source model considering a landscape to be consisted of bare soil and vegetation to estimate EF from the Ts/vegetation concept (Nishida et al., 2003). ET was then estimated from EF data and a coefficient of determination of around 0.69 between their estimates and SM was obtained for the prototype product based on NOAA/AVHRR data.

Overall, this brief review of the literature illustrates that EF can be estimated from remotely sensed data and can be used satisfactorily to estimate ET. However, the applicability of remotely sensed EF estimation methods to estimate SM is yet to be evaluated. The objectives of this research are to find the best approach to estimate EF from remotely sensed data to be used as the input for models to estimate SM in Canadian Prairies.

Canadian Prairies are located in the northern region of North American Great Plains and are characterized by semi-arid to sub humid climate. The three Prairie Provinces (Alberta, Saskatchewan and Manitoba) account for approximately 80% of Canada's cropland area, making them agriculturally, socio-economically and environmentally important. However, the area is prone to drought conditions due to its location on the leeward side of the Rocky Mountains, and its distance from the moderating influence of large water bodies. The region is divided by soil-climatic zones, with a brown soil zone in the arid regions in southeastern Alberta and southwestern Saskatchewan, a dark brown soil zone surrounding the brown soil zone; a black soil zone surrounding this dark brown zone covering southern Manitoba and mid-latitude areas of Alberta and Saskatchewan; and a gray and dark gray soil zone covering the northern areas of the agricultural extent of all three provinces (Champagne et al., 2010). The southwestern Canadian Prairies are semi-arid receiving on average around 350–400 mm of precipitation annually with the majority falling between April and June and are highly prone to frequent and severe droughts. The eastern section of the Canadian Prairies has higher amounts of precipitation and contains several large lakes such as Lake Winnipeg and several large rivers.

Studies on the application of passive microwave data for SM estimation in Canadian Prairies have been carried out (Champagne et al., 2011; Champagne et al., 2012) but fewer attempts have evaluated the use of optical/thermal infrared remote sensing methods alone or in combination with passive microwave methods to obtain SM maps (Hassan et al., 2007). Here, the evaporative fraction is first estimated based on Jiang and Islam (2001) with modifications applicable to the study region. Three different combinations of a vegetation index and surface temperature are evaluated for obtaining the Priestley–Taylor parameter which is used for EF and eventually SM estimation. Two new approaches are presented and the results are compared with estimates obtained by a previously improved EF estimation method (Wang et al., 2006). Two different empirical models to obtain SM from EF are also tested and discussed and correlation analysis is performed between estimated and field measured SM data to find the most accurate soil moisture estimation approach.

2. Study area and data

The study area covers parts of Canadian Prairies over Saskatchewan and Alberta (Fig. 1). The study area has semi-arid continental climate with cold winters and warm summers. Most of the precipitation occurs in May to July and averages around 350 mm annually. The orange inset in Fig. 1 located near Saskatoon, SK, shows the region where field data were used to validate the results. This encompasses a network of soil moisture probes installed by the University of Guelph. The network consists of 16 stations with soil moisture monitoring probes installed horizontally at depths of 5, 20 and 50 cm. For this analysis, surface soil moisture from the 5 cm probe was used to match those estimated by the techniques described below. Further description of the region and instrumentation can be found in Champagne et al. (2010) and Magagi et al. (2013). Over the soil moisture network locations the soil moisture probes (Stevens Vitel Hydra Probe II) have been field calibrated to accuracy of ±3% soil moisture. The values were quality checked to remove unrealistically extreme values. SM data covered the period between May 1st 2008 and October 31st 2008 with no data available from end of June to mid August. On average, 11 stations were operating for each day.

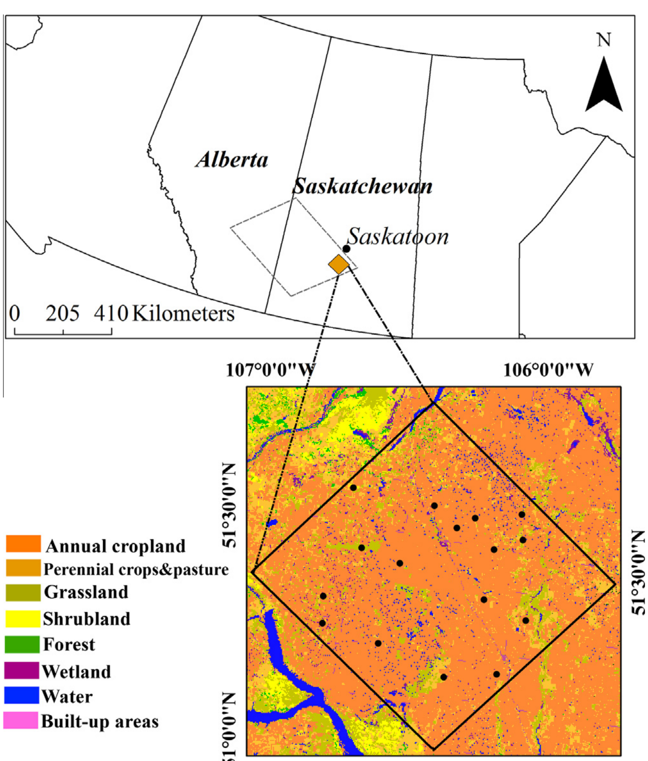

Fig. 1. The study area with the locations of soil moisture measurement stations and land cover composition.

Satellite data used in this study were MODIS Terra (10:30 am) and Aqua (1:30 am, 1:30 pm) daily surface temperature having 1 km resolution (MOD11A1 and MYD11A1, respectively) and MODIS Terra 7-day NDVI composite product supplied by Agriculture and Agri-food Canada (AAFC) retrieved from daily 250 m surface reflectance data (MOD09GQ). For this research, MODIS Terra-day and Aqua-day surface temperatures for four days during growing season (DOY 137, 148, 232 and 260) and MODIS Aqua-night for 3 days (DOY 148, 232 and 260) were selected. This was done to obtain three cloud free images per day for the days with available soil moisture data and to cover a wide range of vegetation condition and enable us to have a comparison between the performances of the three different approaches to estimate EF and SM on the same days.

Air temperature data were obtained from the National Center for Atmospheric Environmental Prediction (NCEP)/North America Regional Reanalysis (NARR) having 32 km spatial resolution and 3 h temporal resolution. Air temperature data at the height of 2 m were used in this research. NAAR data have been shown to provide reasonable estimations of air temperature and precipitation (Choi et al., 2009; Keshta and Elshorbagy, 2011). We revalidated air temperature data with available climatic data in Saskatchewan (10 meteorological stations) in DOY 2008-148 and 260 during MODIS Aqua and Terra satellite overpasses and found accuracies around ±0.6 °C ($R^2 = 0.97$, p-value < 0.0001). Compared to NCEP/National Center for Atmospheric Research (NCAR) data, NAAR data have better spatial resolution and show better correlations with in situ observations (Mesinger et al., 2006; Nigam and Ruiz-Barradas, 2006). Wind speed data were also needed for one of the SM models (Komatsu, 2003) evaluated in this study. However, the NARR data have been shown to underestimate wind speed values (Rasmussen et al., 2011). Therefore, station based meteorological data of wind speed were used for this research. All imagery used in this research was resampled to 500 m resolution before performing the analyses.

3. Methodology

3.1. EF estimation

EF defined as the ratio of ET to available energy can be directly estimated from the last part of the Eq. (1) (Jiang and Islam, 2001):

$$EF = \frac{LE}{R_n - G} = \phi \frac{\Delta}{\Delta + \gamma} \tag{1}$$

where LE is a representative of ET (Wm^{-2}), R_n is the net radiation (Wm^{-2}), G is the soil heat flux and ϕ is the so-called Priestley–Taylor parameter, which is slightly different from the original Priestley–Taylor's parameter (α) as α is generally applicable for wet surfaces whereas ϕ can be applied for a wide range of surface evaporative conditions (Jiang and Islam, 2001). Δ is the slope of saturated vapor pressure and air temperature (Ta) (hPa K^{-1}) and γ is the psychometric constant having the same dimension as Δ. The term $\Delta/(\Delta + \gamma)$ also called the air temperature control parameter varying between 0.55 and 0.85 for air temperatures between 10 and 40 °C is used to normalize the EF so that the seasonal variation of air temperature can be partly removed and better relationships between soil moisture and EF can be established (Wang et al., 2006). For the purpose of this research, Δ and γ were calculated using the relationships given by WMO (2008) (WMO, 2008) and NARR data for air temperature.

Assuming that there are physical relationships between ϕ, SM, Ts and vegetation index or fraction (F_{veg}), ϕ can be estimated through the Ts/vegetation space from remote sensing data as explained in the next section.

3.2. The Ts/NDVI method

As presented in the Introduction, the triangular/trapezoidal shape of the data falling between the Ts and the NDVI has been documented by a number of studies. The lower edge of this space (Wet edge) is characterized by wet land surfaces with maximum evapotranspiration whereas the upper edge (Dry edge) of the scatter plot represents dry land with limited evapotranspiration. Of note, the surface temperature axis in the Ts/NDVI space described above is a simplified term of Ts−Ta which is the difference between surface temperature and air temperature mostly seen as a trapezoidal shape (Moran et al., 1994). Ts−Ta is a representative of energy exchange at the earth surfaces and is linearly related to Vapour Pressure Deficit (VPD) (Idso et al., 1981; Jackson et al., 1981). Ts−Ta is often replaced by Ts due to lack of air temperature data especially for large areas. However, when using the Ts instead of Ts−Ta to estimate soil moisture status, heterogeneity of the earth surfaces increases the uncertainty of the method to estimate SM (Rahimzadeh-Bajgiran et al., 2012). Therefore, the Ts/NDVI method should ideally be applied over smaller regions and those with little topographic variation.

Stisen et al. (2008) and Wang et al. (2006) also considered temporal variations of Ts (day-night Ts differences) instead of only using Ts in the temperature axis of the scatter plot to better estimate EF. The diurnal Ts difference has a similar concept to that of thermal inertia; as soil thermal inertia relates to SM, it can be applied to SM estimation as well (Cai et al., 2007; Verstraeten et al., 2006).

In Jiang and Islam (2001) model, ϕ can be estimated through the Ts/vegetation space from remote sensing data. In this research, ϕ is estimated by three different combinations of temperatures and NDVI is replaced by vegetation fraction. The schematic presented in Fig. 2 was used to estimate ϕ values. Three different variables were examined to be used as the *y* axis; (1) Ts−Ta where Ts is derived from MODIS Terra-day acquisition, (2) Ts−Ta where Ts is derived from MODIS Aqua-day acquisition and (3) ΔTs where the difference between day and night temperatures of MODIS Aqua was used. Terra-day, Aqua-day and Aqua-night Ts values correspond to 10:30 am, 1:30 pm and 1:30 am measurement times, respectively. Ta is NARR 3-h average air temperature around satellite overpass times. The ΔTs approach (Approach 3) was previously developed by Wang et al. (2006) and had provided improved relationships with field measured EF than the original model (Jiang and Islam, 2001) and therefore has been used here as a reference to compare with our approaches. The *x* axis of the scatter plot is vegetation fraction as calculated from NDVI values according to Gillies and Carlson (1995) where $NDVI_{min}$ and $NDVI_{max}$ were 0.11 and 0.87, respectively.

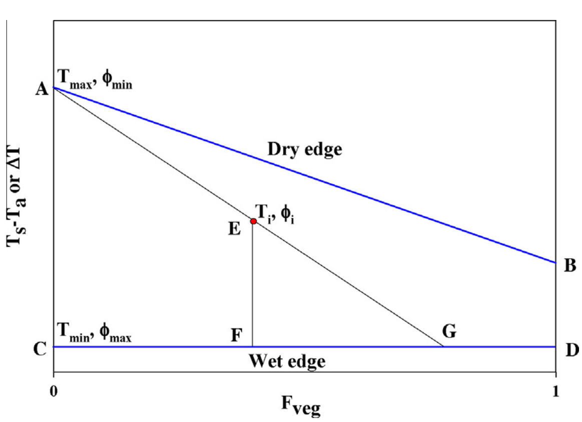

Fig. 2. Theoretical space between temperature and vegetation fraction.

In the scatter plot presented schematically in Fig. 2, the lower edge of the space (Wet edge = CD) is representative of wet land covers with maximum evapotranspiration whereas the upper edge (Dry edge = AB) of the scatter plot represents dry land covers with reduced evapotranspiration. The ϕ value ranges between zero (ϕ_{min}) for zero vegetation fraction with maximum temperature and 1.26 (ϕ_{max}) for maximum vegetation fraction and minimum temperature. The ϕ value for each pixel *i* (e.g. *E*(Ts−Ta/F_{veg}) is calculated by connecting point *A* to point *E* and extending it to point *G*. The ϕ value at point *A* is equal to ϕ_{min} and the wet edge has the maximum ϕ_{max}. Therefore, the length of line AG will be equal to $\phi_{max}-\phi_{min}$ whereas AE will be $\phi_i-\phi_{min}$. Using the similarity of triangles EFG and ACG, ϕ_i at any point in the scatter plot can be calculated as:

$$\phi_i = \frac{T_{\max} - T_i}{T_{\max} - T_{\min}}(\phi_{\max} - \phi_{\min}) + \phi_{\min} \tag{2}$$

where *T* is Ts−Ta or ΔTs in the scatter plot. Details on the calculation procedure for each pixel using this two-step linear interpolation method are described elsewhere (Jiang and Islam, 2001; Tang et al., 2010; Venturini et al., 2004; Wang et al., 2006). Finally Eq. (1) was used to calculate EF values.

3.3. Soil moisture estimation from EF

For soil moisture estimation using satellite data it is crucial to select a model that can best correlate remotely sensed EF to soil moisture. Here we used the Komatsu (2003) and Lee and Pielke (1992) models for the estimation of soil moisture from EF data.

Komatsu (2003) suggested a relationship to describe EF based on soil moisture:

$$EF = 1 - \exp(-\theta/\theta_c) \tag{3}$$

where EF is the evaporative fraction, θ is the volumetric soil moisture and θ_c is the characteristic volumetric water content depending on the soil type and wind speed calculated using:

$$\theta_c = \theta_{c0}(1 + \gamma/r_a) \tag{4}$$

where θ_{c0} and γ are two soil dependent parameters estimated from Komatsu (2003) and r_a is the aerodynamic resistance over bare soil determined using wind speed and soil roughness data and was considered to be 0.005 m for bare soil (Nishida et al., 2003).

The second model is suggested by Lee and Pielke (1992) as presented in:

$$EF = \begin{cases} \frac{1}{4}\left[1 - \cos\left(\frac{\theta}{\theta_{fc}}\pi\right)\right]^2 & \theta < \theta_{fc} \\ 1 & \theta \geqslant \theta_{fc} \end{cases}$$

where θ and θ_{fc} are the volumetric soil moisture and the volumetric soil moisture at field capacity, respectively. Assuming that all different soils should behave the same at some fixed soil-water characteristics, a reference point (soil field capacity) is used in this model. Based on the soil texture of the study area varying from silt loam and clay loam, θ_{fc} was assumed to be 0.3 and 0.35 vol/vol, respectively (Saxton and Rawls, 2006). The application of both models is assessed in discussion below.

3.4. Estimated and observed soil moisture correlation

The estimated SM data obtained through all three approaches were correlated with field measured SM values using Pearson's correlation analysis. Confidence and prediction bands at 95% confidence level were calculated based on Scheffé method (Scheffé, 1999) within Sigmaplot® software. Root Mean Square Error (RMSE) values for all three approaches were also calculated as a measure of the accuracy of the estimations.

4. Results

4.1. Comparing EF estimations retrieved from three different approaches

Sample scatter plots of vegetation fraction and temperature difference for the three approaches namely, Ts−Ta Terra-day, Ts−Ta Aqua-day and ΔTs Aqua-DayNight used in this study are presented in Fig. 3 for the same day (DOY 2008-148). All scatter plots represent the trapezoidal shape described by Moran et al. (1994). Very similar scatter plots are seen for Ts−Ta/F_{veg} derived from Terra day and Aqua day data. On the other hand, the scatter plot for the ΔTs Aqua-DayNight/F_{veg} shows both wider range and higher values as compared with the other two scatter plots. The Ts−Ta/F_{veg} scatter plot for Terra day data constructed here is similar to that presented by Rahimzadeh-Bajgiran et al. (2012), which was used for the estimation the improved Temperature Vegetation Dryness Index (iTVDI). The scatter plot for ΔTs Aqua-Day-Night/F_{veg} resembles that reported by Wang et al. (2006) used to estimate EF.

EF maps calculated using Eq. (1) for 2 days (DOY 2008-148 and DOY 2008-260) for the 60 km by 60 km area with soil moisture data are presented in Fig. 4. The fundamental relationships existing between satellite derived EF and field measured EF have been previously established for Ts/NDVI method (Jiang and Islam, 2001; Venturini et al., 2004) and ΔTs/NDVI (Stisen et al., 2008; Wang et al., 2006). Therefore, our discussion will be limited to the comparison of our suggested approaches to retrieve EF from satellite data with the reference ΔTs approach to find the most appropriate one for soil moisture estimation over this study region.

For all days studied in this research, the Aqua-day approach resulted in the highest estimated EF values whereas those derived from the Aqua-DayNight approach exhibited the lowest values.

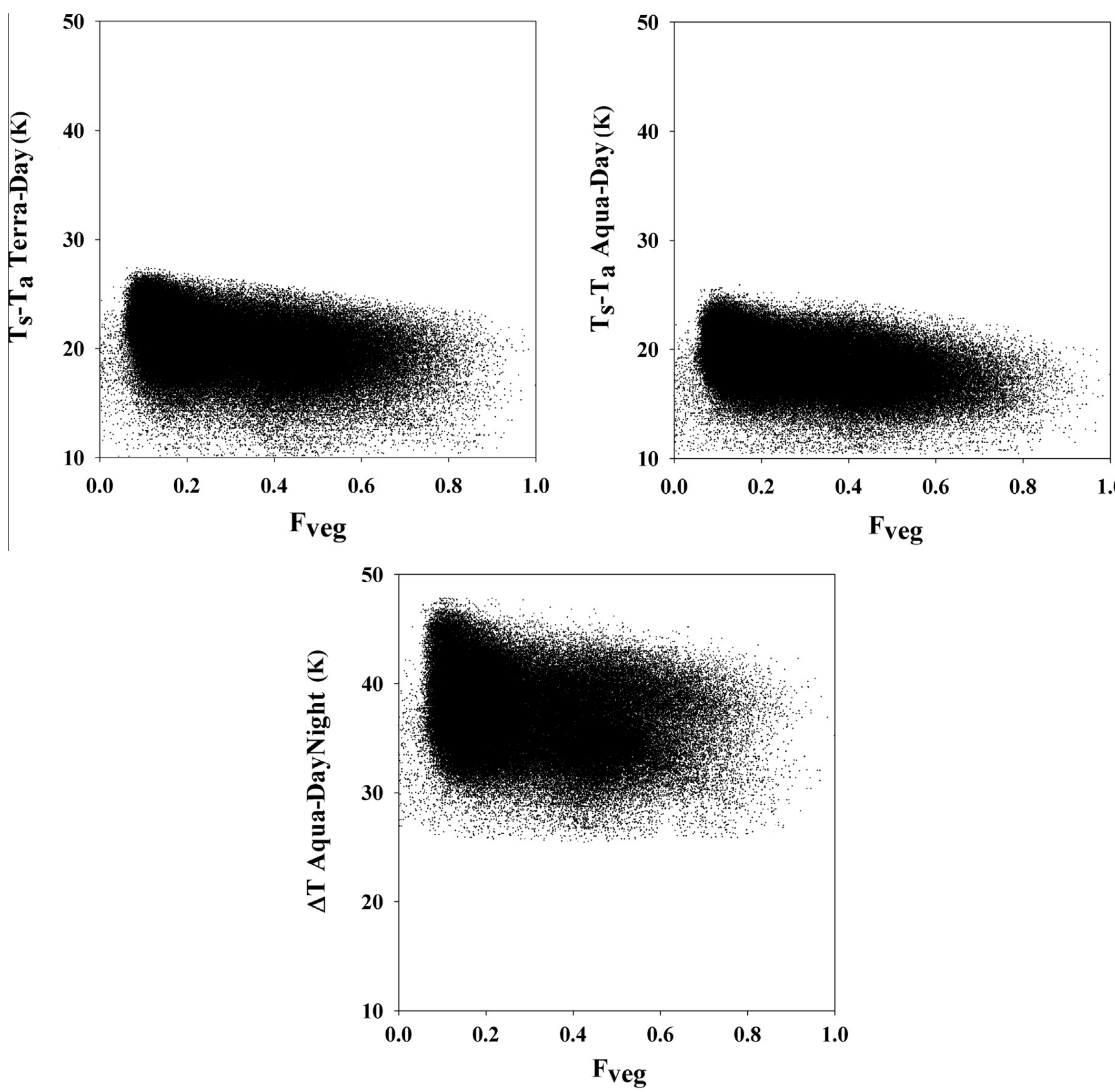

Fig. 3. Examples of scatter plots of vegetation fraction and the three different temperature combinations evaluated in this study (data from DOY 2008-148).

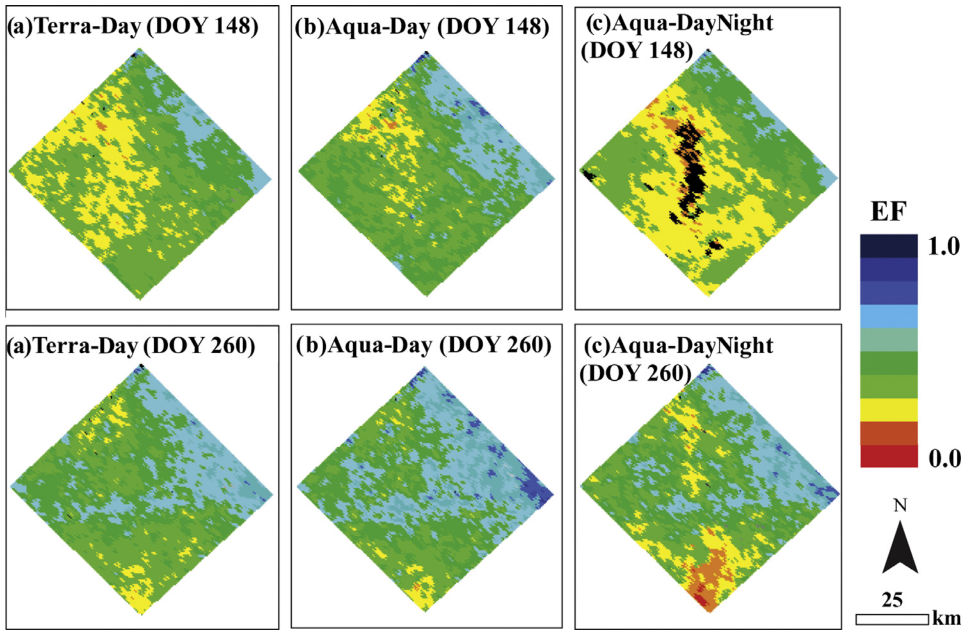

Fig. 4. Comparison of EF maps retrieved through three different approaches for DOY 2008-148 and DOY 2008-260.

The Terra-day approach gave intermediate values. This trend is clearly seen in Fig. 4 for DOY 2008-148 and DOY 2008-260 where all three approaches exhibit similar trends.

4.2. Soil moisture estimation from evaporative fraction

A simulated representation of the Komatsu (2003) and Lee and Pielke (1992) models along with data points for Terra-day and Aqua-day estimated EF and field soil moisture values for 2 days (DOY 2008-137 and DOY 2008-148) is presented in Fig. 5. It was observed that our data were better fitted to the cosine model (Eq. (5)) presented by Lee and Pielke (1992) whereas the Komatsu (2003) exponential model (Eq. (3)) resulted in very low SM estimations for all EF values. As an example, the EF value of 0.6 results in SM values of less than 0.1 vol/vol and around 0.2 vol/vol, using Eqs. (3) and (5), respectively which is closer to data retrieved from MODIS for the latter. As explained by Komatsu (2003), this model is more appropriate for wet soils in thin layers and the shape of the curve approaches that of Lee and Pielke (1992) at higher soil depths. Therefore, Eq. (5) was used in the present study to estimate SM from EF.

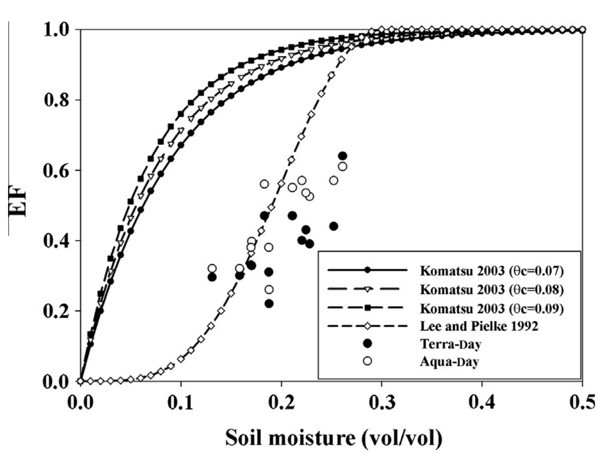

Fig. 5. Theoretical representation of EF/SM relationships used in the present study. θ_c in Komatsu (2003) for agricultural soil ranges between 0.07 and 0.09 based on varying wind speeds of 2–6 m/s. θ_{fc} is 0.3 vol/vol for Lee and Pielke (1992).

4.3. Correlations between estimated soil moisture and field data

Results of correlation analyses performed between estimated SM data obtained from Eq. (5) and field measurements for the three different approaches in days DOY 2008-137, 148, 232 and 260 are presented in Fig. 6 and corresponding data are tabulated in Table 1. Aqua-DayNight data for DOY 2008-137 were not available due to cloud contamination. All three approaches resulted in statistically significant correlations between estimated and observed SM for all days. For each day, estimated SM obtained from Ts−Ta Aqua-day generally had better correlations with field data confirmed by higher coefficients of determination. This is in agreement with Fig. 5 where Aqua-day data points are better distributed around the cosine curve. SM values estimated from ΔTs Aqua-DayNight resulted in the lowest R^2 values compared with the other two approaches.

Coefficients of determination were found to be higher for DOY 137 and DOY 148 as compared with the other 2 days. This can be attributed to the amount of vegetation fraction whose variations are presented in Fig. 7 for all days. As it can be seen, vegetation fraction is the highest for DOY 2008-232 where the lowest R^2 values were obtained.

Average RMSE values for the three approaches of estimations and various days ranged between 3.9 and 6.9 vol/vol%. However, as presented in Fig. 8 where square errors for all days and approaches are plotted versus field SM data, the highest errors of estimation correspond to high and low SM values where the number of samples were limited. Intermediate SM values in the range of 12–22 vol/vol% resulted in square errors averaging lower than 11 $(\text{vol/vol\%})^2$ and consequently more accurate estimations.

5. Discussion

The analysis of EF values obtained from the three studied approaches showed similar trends for each day but slightly higher values for the Ts−Ta Aqua-day approach. On the other hand, the

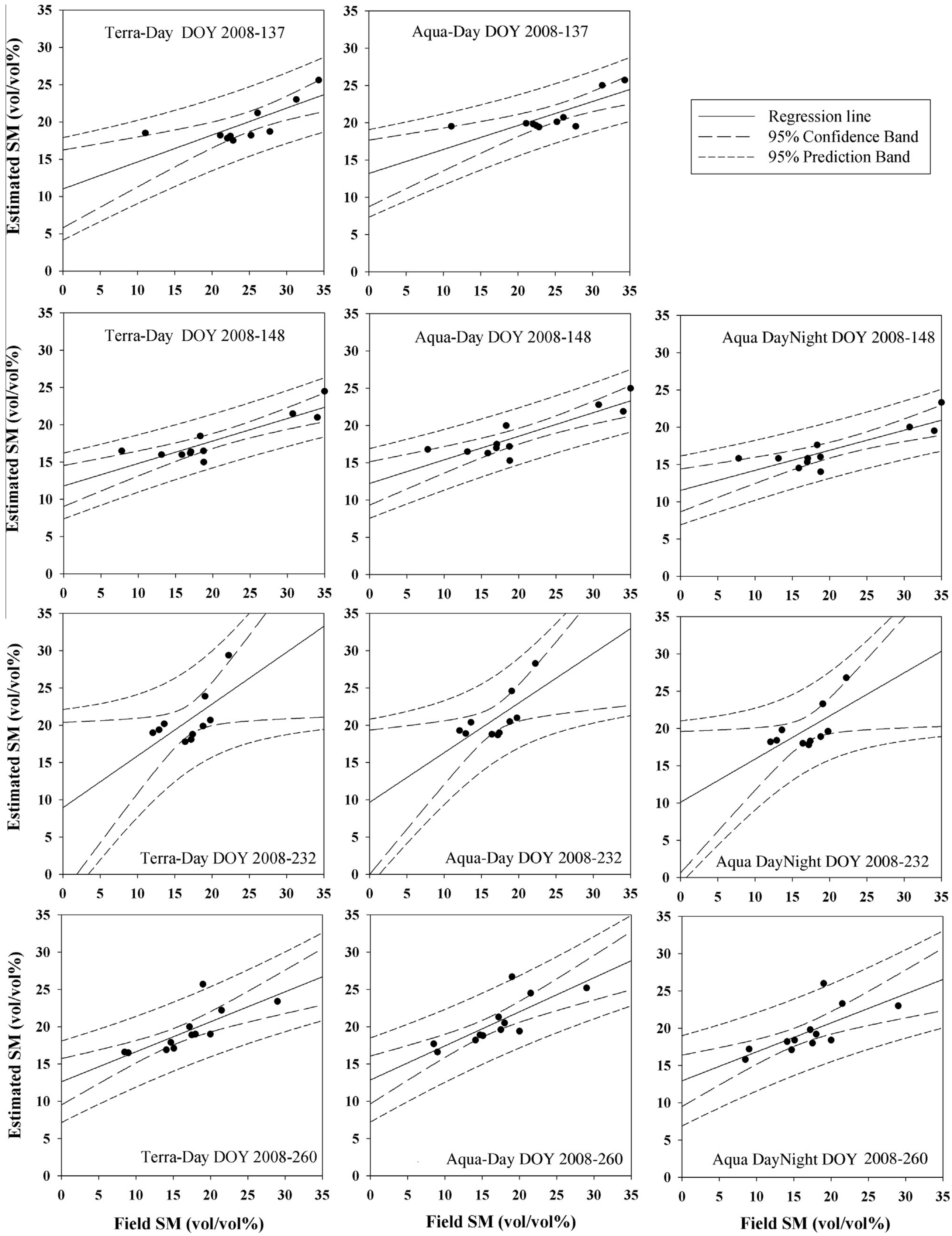

Fig. 6. Correlations between MODIS estimated and observed SM data.

ΔTs Aqua-DayNight approach gave slightly lower EF values. The EF estimated from Terra-day can be considered to be equivalent to mid morning EF whereas that from Aqua-day represents noon or early afternoon EF. Therefore, the slight variations observed in estimated EF values derived from different approaches can be attributed to the overpass time of the satellite data. However, previous

Table 1
Coefficients of determination (R^2), statistical significance (p value), and average root mean square errors ($RMSE_{ave}$) for each day and satellite data combination.

Approach	Satellite data	DOY	R^2	p Value	$RMSE_{ave}$ (vol/vol%)
Ts−Ta	Terra-day	137	0.66	0.0025	6.9
	Aqua-day	137	0.67	0.0019	6.4
ΔTs	Aqua-DayNight	137	–	–	–
Ts−Ta	Terra-day	148	0.77	0.0004	6.5
	Aqua-day	148	0.77	0.0004	6.2
ΔTs	Aqua-DayNight	148	0.71	0.0012	7.2
Ts−Ta	Terra-day	232	0.42	0.0425	4.6
	Aqua-day	232	0.48	0.0259	4.7
ΔTs	Aqua-DayNight	232	0.42	0.0417	3.9
Ts−Ta	Terra-day	260	0.57	0.0046	4.4
	Aqua-day	260	0.61	0.0025	5.0
ΔTs	Aqua-DayNight	260	0.50	0.0101	4.6

studies indicate that contrary to ET, EF does not significantly vary during the day and that noon time EF values can be considered to be equivalent to daily EF (Crago, 1996). The ΔTs Aqua-DayNight approach had been previously proposed as an alternative to improve the accuracy of EF estimation as compared with Jiang and Islam model which only uses Ts in the y axis of the scatter plot (Wang et al., 2006). Our estimated EF values were found to be slightly higher when air temperature was included in the model (Ts−Ta Terra-day and Aqua-day). That which EF estimation approach could be used more accurately to estimate SM would however depend on the correlations between estimated and field measured soil moisture.

The accuracy of SM estimation from EF values as retrieved from satellite data depends on the accuracy of EF estimation from the scatter plots as well as the performance of the equation used to convert EF to SM. Previous studies have obtained satisfactory results correlating measured ground EF to estimated EF values providing a good alternative for large areas with limited field data (Jiang and Islam, 2001; Venturini et al., 2004; Wang et al., 2006). The accuracy of EF estimation in turn depends on accurate determination of wet and dry edges used to calculate EF for each pixel. We selected a relatively larger area than the area with field soil moisture data to establish wet and dry edges more accurately. This makes it easier to find pixels with extreme SM values to be included in the scatter plot especially following rainfall. In addition, the threshold used for identifying bare soil pixels could be set more accurately in a larger area. On the other hand, by incorporating air temperature in the model using NARR Ta data we tried to minimize errors caused by selecting too large an area with possible topography variations. However, these simplified models for the estimation of EF from satellite data are based on a number of assumptions making them sensitive to different sources of error as described by other authors (Jiang and Islam, 2001; Sandholt et al., 2002).

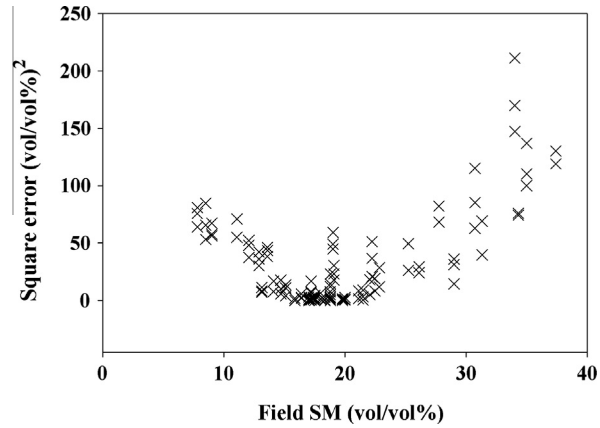

Fig. 8. Square errors of the estimation of SM as a function of observed SM values.

The model to be used for converting EF data to SM values will also have an important role in the accuracy of SM estimation. The Komatsu (2003) model was found to be unsuitable for the estimation of SM from MODIS derived EF after initial analysis.

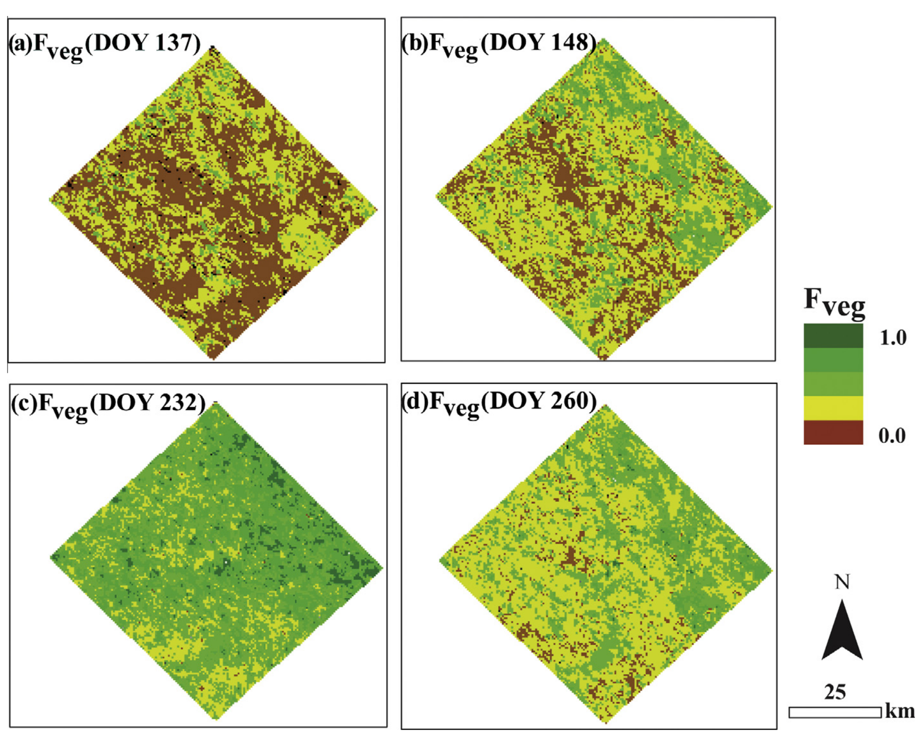

Fig. 7. Changes in vegetation fraction over the study period.

Although this model includes more variables than the Lee and Pielke's model taking into account wind speed as well, the main reason for its unsuitability for our data can be attributed to the fact that it is based on soil thickness of only 1 mm. Komatsu (2003) indicated that at higher soil thicknesses the relationship approaches that of the cosine curve but no model parameters were developed by the author for deeper soils appropriate for our purpose. The Lee and Pielke (1992) model showed better results providing reasonable estimations for intermediate soil moistures but failed to accurately work for low and high SM values resulting in relatively large average RMSEs. Although the true value of θ_{fc} can affect the SM estimation using this model, the accuracy of estimations could also be improved by having a greater number of field SM measurements covering extreme values.

DOY 2008-148 and 2008-137 were found to present higher correlations between estimated and field measured SM in all approaches. Both DOY 2008-148 and 2008-137 represent the situation in early growing season in which vegetation fraction is low and EF is more related to soil than vegetation. DOY 2008-232 in which the highest vegetation fraction is observed, exhibited the lowest coefficients of determination, although the relationship is statistically significant. DOY 2008-260 shows a situation in which vegetation fraction is relatively high but on the decline resulting in improvements in correlations between estimated and measured SM as compared with DOY 2008-232. As the relationship between EF and SM is dependent on the depth of SM, which is in turn related to the root depth of the vegetation, empirical models to convert EF data to SM values generally work better for bare soil and shallowly rooted plant covers (Davies and Allen, 1973).

Though not considerably different, the best correlations between field SM and estimated SM data in this research (observed as higher coefficients of determination and more or less similar RMSE values) were obtained when the Ts−Ta Aqua-day and Terra-day approaches were used in all studied days. This indicates that incorporating NARR Ta data into the model both for Terra-day and Aqua-day approaches resulted in better EF estimations thereby providing improved accuracy of SM estimations from EF. One other important advantage of using Ts−Ta approaches over ΔTs is that the former only needs one satellite observation which is a considerable advantage as having two cloud free images over the same area in 24 h can be not very easy in our study area, which was normally cloudy at nights during the study period. The lower R^2 values obtained for the ΔTs approach may also be caused by the cloud contamination of Ts as there is a higher possibility to have a thin cloud cover when using both day and night surface temperature images (see Fig. 4c).

6. Conclusion

In this research, we tried to use the relationship between evaporative fraction and soil moisture to estimate soil moisture from remote sensing data in Canadian Prairies. Three different approaches to estimate EF based on Jiang and Islam (2001) model and two models to estimate soil moisture from EF were evaluated. It was found that SM can be estimated from remotely sensed EF data over the study area. The concept of incorporating air temperature using NARR data into the spatial variation of surface temperature and vegetation fraction was found to improve soil moisture estimation accuracy based on evaporative fraction. Evaluation of models used to estimate soil moisture from EF revealed that at least for the satellite data used in this study, the equation presented by Lee and Pielke (1992) better predicts soil moisture variations based on EF. Among the EF estimation approaches, the Ts−Ta MODIS Aqua-day approach provided more satisfactory results with strong statistically significant correlations between estimated and observed soil moisture data. The accuracy of the predictions was considerably better for intermediate soil moisture values promising the applicability of the method for estimating soil moisture in Canadian Prairies as well as exhibiting the need for further development of the model to account for extreme conditions. However, further work is required to improve the accuracy of the model used to convert EF values to soil moisture for any given set of SM and satellite derived EF thereby improving the overall accuracy of soil moisture estimation. Having obtained statistically significant relationships between soil moisture data derived from MODIS optical/thermal infrared imagery and observed values, the next step would be incorporating the present methodology into downscaling algorithms for passive microwave SM data to benefit from the higher accuracy available from passive estimates but the higher spatial resolution available from the methods described here.

Acknowledgments

Funding from Environment Canada and the Canadian Space Agency supported this research. Jonathon Belanger is acknowledged for his work with the collection and analysis of data from the soil moisture monitoring networks. The constructive comments from three anonymous reviewers were greatly appreciated and improved the quality of this paper.

References

Anderson, M.C., Norman, J.M., Mecikalski, J.R., Otkin, J.A., Kustas, W.P., 2007. A climatological study of evapotranspiration and moisture stress across the continental United States based on thermal remote sensing: 2. Surface moisture climatology. Journal of Geophysical Research-Atmospheres 112, D11112.
Bartholic, J.F., Wiegand, C.L., Namken, L.N., 1972. Aerial thermal scanner to determine temperatures of soils and of crop canopies differing in water stress. Agronomy Journal 64, 603–608.
Cai, G., Xue, Y., Hu, Y., Wang, Y., Guo, J., Luo, Y., Wu, C., Zhong, S., Qi, S., 2007. Soil moisture retrieval from MODIS data in Northern China Plain using thermal inertia model. International Journal of Remote Sensing 28, 3567–3581.
Carlson, T., 2007. An overview of the "triangle method" for estimating surface evapotranspiration and soil moisture from satellite imagery. Sensors 7, 1612–1629.
Carlson, T.N., Capehart, W.J., Gillies, R.R., 1995a. A new look at the simplified method for remote-sensing of daily evapotranspiration. Remote Sensing of Environment 54, 161–167.
Carlson, T.N., Gillies, R.R., Schmugge, T.J., 1995b. An interpretation of methodologies for indirect measurement of soil-water content. Agricultural and Forest Meteorology 77, 191–205.
Champagne, C., Berg, A.A., Belanger, J., McNairn, H., de Jeu, R., 2010. Evaluation of soil moisture derived from passive microwave remote sensing over agricultural sites in Canada using ground-based soil moisture monitoring networks. International Journal of Remote Sensing 31, 3669–3690.
Champagne, C., McNairn, H., Berg, A.A., 2011. Monitoring agricultural soil moisture extremes in Canada using passive microwave remote sensing. Remote Sensing of Environment 115, 2434–2444.
Champagne, C., Berg, A.A., McNairn, H., Drewitt, G., Huffman, T., 2012. Evaluation of soil moisture extremes for agricultural productivity in the Canadian Prairies. Agricultural and Forest Meteorology 165, 1–11.
Chauhan, N.S., Miller, S., Ardanuy, P., 2003. Spaceborne soil moisture estimation at high resolution: a microwave-optical/IR synergistic approach. International Journal of Remote Sensing 24, 4599–4622.
Choi, W., Kim, S.J., Rasmussen, P.F., Moore, A.R., 2009. Use of the North American regional reanalysis for hydrological modelling in Manitoba. Canadian Water Resources Journal 34, 17–36.
Crago, R.D., 1996. Comparison of the evaporative fraction and the Priestley–Taylor alpha for parameterizing daytime evaporation. Water Resources Research 32, 1403–1409.
Davies, J.A., Allen, C.D., 1973. Equilibrium, potential and actual evaporation from cropped surfaces in Southern Ontario. Journal of Applied Meteorology 12, 649–657.
Deardorff, J.W., 1978. Efficient prediction of ground surface-temperature and moisture, with inclusion of a layer of vegetation. Journal of Geophysical Research-Oceans and Atmospheres 83, 1889–1903.
Gillies, R.R., Carlson, T.N., 1995. Thermal remote-sensing of surface soil-water content with partial vegetation cover for incorporation into climate-models. Journal of Applied Meteorology 34, 745–756.
Gillies, R.R., Carlson, T.N., Cui, J., Kustas, W.P., Humes, K.S., 1997. A verification of the 'triangle' method for obtaining surface soil water content and energy fluxes

from remote measurements of the Normalized Difference Vegetation Index (NDVI) and surface radiant temperature. International Journal of Remote Sensing 18, 3145–3166.
Hassan, Q.K., Bourque, C.P.A., Meng, F.-R., Cox, R.M., 2007. A wetness index using terrain-corrected surface temperature and normalized difference vegetation index derived from standard MODIS products: an evaluation of its use in a humid forest-dominated region of eastern Canada. Sensors 7, 2028–2048.
Heilman, J.L., Kanemasu, E.T., Rosenberg, N.J., Blad, B.L., 1976. Thermal scanner measurement of canopy temperatures to estimate evapo transpiration. Remote Sensing of Environment 5, 137–145.
Idso, S.B., Jackson, R.D., Pinter, P.J., Reginato, R.J., Hatfield, J.L., 1981. Normalizing the stress-degree-day parameter for environmental variability. Agricultural Meteorology 24, 45–55.
Jackson, R.D., Idso, S.B., Reginato, R.J., 1976. Calculation of evaporation rates during transition from energy-limiting to soil-limiting phases using albedo data. Water Resources Research 12, 23–26.
Jackson, R.D., Idso, S.B., Reginato, R.J., Pinter, P.J., 1981. Canopy temperature as a crop water-stress indicator. Water Resources Research 17, 1133–1138.
Jacquemin, B., Noilhan, J., 1990. Sensitivity study and validation of a land surface parameterization using the Hapex-Mobilhy data set. Boundary-Layer Meteorology 52, 93–134.
Jiang, L., Islam, S., 2001. Estimation of surface evaporation map over southern Great Plains using remote sensing data. Water Resources Research 37, 329–340.
Keshta, N., Elshorbagy, A., 2011. Utilizing North American regional reanalysis for modeling soil moisture and evapotranspiration in reconstructed watersheds. Physics and Chemistry of the Earth 36, 31–41.
Komatsu, T.S., 2003. Toward a robust phenomenological expression of evaporation efficiency for unsaturated soil surfaces. Journal of Applied Meteorology 42, 1330–1334.
Kondo, J., Saigusa, N., Sato, T., 1990. A parameterization of evaporation from bare soil surfaces. Journal of Applied Meteorology 29, 385–389.
Lee, T.J., Pielke, R.A., 1992. Estimating the soil surface specific-humidity. Journal of Applied Meteorology 31, 480–484.
Li, Z.L., Tang, R., Wan, Z., Bi, Y., Zhou, C., Tang, B., Yan, G., Zhang, X., 2009. A review of current methodologies for regional evapotranspiration estimation from remotely sensed data. Sensors 9 (5), 3801–3853.
Magagi, R., Berg, A.A., Goita, K., Belair, S., Jackson, T.J., Toth, B., Walker, A., McNairn, H., O'Neill, P.E., Moghaddam, M., Gherboudj, I., Colliander, A., Cosh, M.H., Burgin, M., Fisher, J.B., Kim, S.-B., Mladenova, I., Djamai, N., Rousseau, L.-P.B., Belanger, J., Shang, J., Merzouki, A., 2013. Canadian experiment for soil moisture in 2010 (CanEx-SM10): overview and preliminary results. IEEE Transactions on Geoscience and Remote Sensing 51, 347–363.
Mallick, K., Bhattacharya, B.K., Patel, N.K., 2009. Estimating volumetric surface moisture content for cropped soils using a soil wetness index based on surface temperature and NDVI. Agricultural and Forest Meteorology 149, 1327–1342.
Merlin, O., Walker, J.P., Chehbouni, A., Kerr, Y., 2008. Towards deterministic downscaling of SMOS soil moisture using MODIS derived soil evaporative efficiency. Remote Sensing of Environment 112, 3935–3946.
Merlin, O., Al Bitar, A., Walker, J.P., Kerr, Y., 2010. An improved algorithm for disaggregating microwave-derived soil moisture based on red, near-infrared and thermal-infrared data. Remote Sensing of Environment 114, 2305–2316.
Mesinger, F., DiMego, G., Kalnay, E., Mitchell, K., Shafran, P.C., Ebisuzaki, W., Jovic, D., Woollen, J., Rogers, E., Berbery, E.H., Ek, M.B., Fan, Y., Grumbine, R., Higgins, W., Li, H., Lin, Y., Manikin, G., Parrish, D., Shi, W., 2006. North American regional reanalysis. Bulletin of the American Meteorological Society 87, 343–360.
Moran, M.S., Clarke, T.R., Inoue, Y., Vidal, A., 1994. Estimating crop water-deficit using the relation between surface-air temperature and spectral vegetation index. Remote Sensing of Environment 49, 246–263.
Moran, M.S., Peters-Lidard, C.D., Watts, J.M., McElroy, S., 2004. Estimating soil moisture at the watershed scale with satellite-based radar and land surface models. Canadian Journal of Remote Sensing 30, 805–826.
Nemani, R., Pierce, L., Running, S., Goward, S., 1993. Developing satellite-derived estimates of surface moisture status. Journal of Applied Meteorology 32, 548–557.
Nigam, S., Ruiz-Barradas, A., 2006. Seasonal hydroclimate variability over North America in global and regional reanalyses and AMIP simulations: varied representation. Journal of Climate 19, 815–837.
Nishida, K., Nemani, R.R., Running, S.W., Glassy, J.M., 2003. An operational remote sensing algorithm of land surface evaporation. Journal of Geophysical Research-Atmospheres 108, D94270.
Njoku, E.G., 1977. Theory for passive microwave remote-sensing of near-surface soil-moisture. Journal of Geophysical Research 82, 3108–3118.
Noilhan, J., Planton, S., 1989. A simple parameterization of land surface processes for meteorological models. Monthly Weather Review 117, 536–549.
Owe, M., de Jeu, R., Holmes, T., 2008. Multisensor historical climatology of satellite-derived global land surface moisture. Journal of Geophysical Research-Earth Surface 113, F01002.
Petropoulos, G., Carlson, T.N., Wooster, M.J., Islam, S., 2009. A review of T-s/VI remote sensing based methods for the retrieval of land surface energy fluxes and soil surface moisture. Progress in Physical Geography 33, 224–250.
Piles, M., Camps, A., Vall-Llossera, M., Corbella, I., Panciera, R., Ruediger, C., Kerr, Y.H., Walker, J., 2011. Downscaling SMOS-derived soil moisture using MODIS visible/infrared data. IEEE Transactions on Geoscience and Remote Sensing 49, 3156–3166.
Price, J.C., 1990. Using spatial context in satellite data to infer regional scale evapotranspiration. IEEE Transactions on Geoscience and Remote Sensing 28, 940–948.
Priestley, C.H.B., Taylor, R.J., 1972. Assessment of surface heat-flux and evaporation using large-scale parameters. Monthly Weather Review 100, 81–92.
Rahimzadeh-Bajgiran, P., Omasa, K., Shimizu, Y., 2012. Comparative evaluation of the Vegetation Dryness Index (VDI), the Temperature Vegetation Dryness Index (TVDI) and the improved TVDI (iTVDI) for water stress detection in semi-arid regions of Iran. ISPRS Journal of Photogrammetry and Remote Sensing 68, 1–12.
Rasmussen, D.J., Holloway, T., Nemet, G.F., 2011. Opportunities and challenges in assessing climate change impacts on wind energy-a critical comparison of wind speed projections in California. Environmental Research Letters 6.
Sandholt, I., Rasmussen, K., Andersen, J., 2002. A simple interpretation of the surface temperature/vegetation index space for assessment of surface moisture status. Remote Sensing of Environment 79, 213–224.
Saxton, K.E., Rawls, W.J., 2006. Soil water characteristic estimates by texture and organic matter for hydrologic solutions. Soil Science Society of America Journal 70, 1569–1578.
Scheffé, H., 1999. The analysis of variance. John Wiley & Sons, New York, 477p.
Schmugge, T., 1978. Remote-sensing of surface soil-moisture. Journal of Applied Meteorology 17, 1549–1557.
Schmugge, T., Jackson, T.J., 1994. Mapping surface soil-moisture with microwave radiometers. Meteorology and Atmospheric Physics 54, 213–223.
Stisen, S., Sandholt, I., Norgaard, A., Fensholt, R., Jensen, K.H., 2008. Combining the triangle method with thermal inertia to estimate regional evapotranspiration – applied to MSG-SEVIRI data in the Senegal River basin. Remote Sensing of Environment 112, 1242–1255.
Tang, R., Li, Z.-L., Tang, B., 2010. An application of the Ts-VI triangle method with enhanced edges determination for evapotranspiration estimation from MODIS data in and and semi-arid regions: Implementation and validation. Remote Sensing of Environment 114, 540–551.
Venturini, V., Bisht, G., Islam, S., Jiang, L., 2004. Comparison of evaporative fractions estimated from AVHRR and MODIS sensors over South Florida. Remote Sensing of Environment 93, 77–86.
Verstraeten, W.W., Veroustraete, F., van der Sande, C.J., Grootaers, I., Feyen, J., 2006. Soil moisture retrieval using thermal inertia, determined with visible and thermal spaceborne data, validated for European forests. Remote Sensing of Environment 101, 299–314.
Verstraeten, W.W., Veroustraete, F., Feyen, J., 2008. Assessment of evapotranspiration and soil moisture content across different scales of observation. Sensors 8, 70–117.
Wang, L., Qu, J.J., 2009. Satellite remote sensing applications for surface soil moisture monitoring: a review. Frontiers of Earth Science in China 3, 237–247.
Wang, K.C., Li, Z.Q., Cribb, M., 2006. Estimation of evaporative fraction from a combination of day and night land surface temperatures and NDVI: A new method to determine the Priestley–Taylor parameter. Remote Sensing of Environment 102, 293–305.
Wang, W., Huang, D., Wang, X.G., Liu, Y.R., Zhou, F., 2011. Estimation of soil moisture using trapezoidal relationship between remotely sensed land surface temperature and vegetation index. Hydrology and Earth System Sciences 15, 1699–1712.
WMO, 2008. Guide to Meteorological Instruments and Methods of Observation. WMO-World Meteorological Organization (CIMO Guide), Geneva.
Yao, Y., Qin, Q., Ghulam, A., Liu, S., Zhao, S., Xu, Z., Dong, H., 2011. Simple method to determine the Priestley–Taylor parameter for evapotranspiration estimation using Albedo-VI triangular space from MODIS data. Journal of Applied Remote Sensing 5, 1–12.